ff

EUROPEAN ORGANIZATION FOR NUCLEAR RESEARCH

CERN–ECP/95–2
20 January 1995

FLUENCE AND DOSIMETRIC MEASUREMENTS FOR A $\pi^{\pm}$ IRRADIATION FACILITY

RD2 Collaboration

C. Furetta, S.J. Bates, M. Glaser, F. Lemeilleur, M. Tavlet
CERN, Geneva, Switzerland

E. León-Florián, C. Leroy
University of Montreal, Montreal, Canada

Abstract

This paper briefly describes the pion irradiation facility used by the SIRAD (Silicon Radiation) Collaboration in mid-1994 at the Paul Scherrer Institute (PSI) in Villigen, Switzerland, and reports the fluence measurements carried out with the Al activation technique during silicon detector irradiations. Calibration factors were determined as a ratio between the fluence and the number of counts from an ionization chamber. Some dosimetric measurements were also performed using alanine and thermoluminescent dosimeters, which allowed the π and the γ dose rates to be determined. ^{115}In activation was also used to determine the neutron contamination around the π-beam.

Presented at the 4th Conference on Advanced Technology and Particle Physics Villa Olmo, October 3–7, 1994, Como, Italy

Fluence and dosimetric measurements for a $\pi^{\pm}$ irradiation facility

RD2 Collaboration

C. Furetta, S.J. Bates, M. Glaser, F. Lemeilleur, M. Tavlet[a]
E. León-Florián, C. Leroy[b]

[a]CERN, Geneva, Switzerland

[b]University of Montreal, Montreal, Canada

This paper briefly describes the pion irradiation facility used by the SIRAD (Silicon Radiation) Collaboration in mid-1994 at the Paul Scherrer Institute (PSI) in Villigen, Switzerland, and reports the fluence measurements carried out with the Al activation technique during silicon detector irradiations. Calibration factors were determined as a ratio between the fluence and the number of counts from an ionization chamber. Some dosimetric measurements were also performed using alanine and thermoluminescent dosimeters, which allowed the π and the γ dose rates to be determined. ^{115}In activation was also used to determine the neutron contamination around the π-beam.

1. INTRODUCTION

The Large Hadron Collider (LHC), operational by the beginning of the next century at CERN, will bring protons into head-on collisions at a centre of mass energy of 14 TeV with an expected peak luminosity of 1.7×10^{34} cm^{-2} sec^{-1}. The LHC operating conditions will create a high-level radiation environment producing radiation damage in detectors and their associated electronic components. Silicon is expected to be used as the active medium for several detectors in the future LHC experiments. As a consequence, detailed studies are under way to understand the behaviour of the silicon detectors in such an adverse environment.

The irradiation modifies the crystalline structure of the silicon detectors as well as their electrical characteristics. The charge collection efficiency is reduced and the leakage current increases. The effective doping concentration also changes. Generally speaking, the degradation phenomena can be described in terms of minority carrier lifetime reduction, acceptor creation and carrier mobility reduction.

The establishment of a correlation between damage and irradiation primarly requires a good understanding of the environmental conditions. This knowledge is provided by a precise determination of the particle fluxes and/or absorbed doses involved during irradiation of the silicon detectors. The aim of this paper is to give a brief description of the pion irradiation facility used by the SIRAD (Silicon Radiation) collaboration in mid-1994 at the Paul Scherrer Institute (PSI), Villigen, and to present the results of the fluence and dosimetric measurements.

2. EXPERIMENTAL SET-UP

The high intensity PSI pion beam (Π-E1) has a momentum range from 100 to 450 MeV/c. Pions, produced by the collision of the cyclotron proton beam with a graphite target, are guided via a beam line down to the irradiation zone. The maximum proton current of the cyclotron is $\sim$ 800 μA. After the production target, the pion beam is contaminated with a large number of protons filtered by means of graphite plate absorbers. Proton interactions in graphite produce a yield of neutrons which must be measured. The lepton contamination of the pion beam at the irradiation position (estimated to be $\sim$ 10%) is expected to induce damage in silicon of at least one order of magnitude lower than that of hadrons [1]. Therefore, the damaging effect of leptons can be safely neglected to a first approximation.

The irradiation position is located $\sim$ 1 m downstream of the last quadrupole magnet at a height of $\sim$ 1.5 m. A sketch of the experimental set up

Table 1
List of the activation detectors used during the pion irradiations and their main characteristics

ACTIVATION DETECTORS						
MATERIAL	AREA (mm^2)	THICKNESS (mm)	REACTION	HALF LIFE ($T_{1/2}$)	γ EMISSION	RADIATION DETECTED
Aluminium	10 × 10 8 × 8 5 × 5 6 × 12	0.1 0.1 0.1 0.1	$^{27}AL(\pi^{\pm},xN)^{24}NA$	15.06 h	1369 keV (99%)	π
Carbon	10 × 10	1	$^{12}C(\pi^{\pm},xN)^{11}C$	20.39 min	511 keV (200%)	π
Indium	28.3	0.3	$^{115}In(n,n')^{115m}In$ $^{115}In(n,\gamma)^{116m}In$	4.50 h 54.0 min	336 keV (46%) 417 keV (29%) 1097 keV (56%) 1294 keV (85%)	n(0.5–14.0 MeV) thermal neutrons

is shown in Fig. 1. An ionizing chamber, an X–Y chamber and a luminescent screen were used to monitor the beam. The ionization chamber was present during the whole period of irradiation and the digitized induced current, N_{ic}, (proportional to the total pion beam intensity) was used to record the fluence during the irradiation periods (see Section 5). The X–Y chamber was moved along the beam direction to measure the vertical and horizontal FWHM beam profile at each position of irradiation. The transverse beam density, expressed as $1/[(FWHM)_H \cdot (FWHM)_V]$, was then calculated at each position. Figure 2 shows the transverse π^+ beam profile and density, as a function of longitudinal position, obtained at 350 MeV/c.

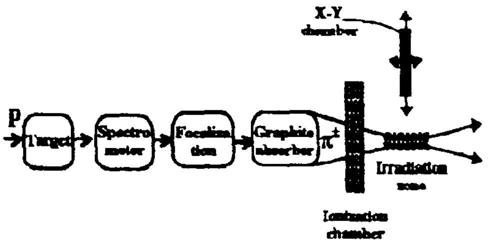

Figure 1. Diagram of the beam and irradiation set-up

The technique of activation was chosen to measure the fluences during the irradiations. The activation detectors and their characteristics are summarized in Table 1. Table 2 lists the type of dosimeters used to estimate gamma and neutron production during the π^+ irradiation.

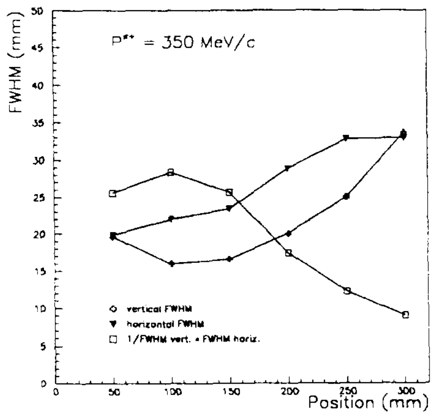

Figure 2. Transverse π^+ beam profile and density versus longitudinal position at a momentum of 350 MeV/c

Figure 3 shows the respective positions of the activation detectors and the dosimeters in the irradiation box.

The activation detectors were Aluminium, Carbon and Indium foils, mounted in cardboard frames. The Al foils had the same area as the detectors to be irradiated and were located in the irradiation box between the groups of silicon detectors. The box was mounted on a table movable in three dimensions (x, y, z) to optimize its position in the beam.

Table 2
List of dosimeters used during the pion irradiation and their main characteristics

DOSIMETERS						
MATERIAL	AREA (mm^2)	THICKNESS (mm)	PHYSICAL EFFECT	TECHNIQUE OF MEASUREMENT	MEASURED QUANTITY	RADIATION DETECTED
LiF:Mg, Ti (TLD-700)	9	0.9	Electron excitation	Heating	Light	γ
Alanine (PAD)	144	Ø4.8	Free radical production	Electron Spin Resonance	Free radical number	π

Thermoluminescent (TLD) and polymer-alanine (PAD) dosimeters were inserted in plastic bags. The TLDs were located out of the beam line because this type of dosimeter is not suitable for high-level dosimetry (the linearity of the absorbed dose is only valid up to about 1 Gy); on the contrary the PADs were positioned in the beam because their dose range is linear up to about 50 kGy. The dose rate due to pions is estimated to be of the order of 180 Gy/h in water and about one order of magnitude lower in silicon.

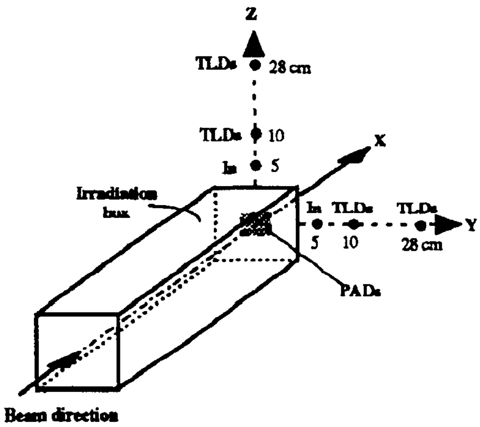

Figure 3. Diagram of the irradiation box and the dosimeter positions

Before irradiation of the silicon detectors, a range of photographic films were exposed in the beam in order to determine the exact position of the beam spot for aligning the irradiation box. The films were fixed at the front and the rear of the box.

3. FLUENCE MEASUREMENTS

The fluence measurement required is the integrated flux of specific particles over the irradiation time. The fluence can be determined from the activity, A, induced in the given materials, and a brief description of the techniques is given below.

3.1. Mathematical treatment

The activity of the irradiated material at the end of the irradiation is given by:

$$A = \varphi \cdot \sigma \cdot N_0[1 - \exp(-\lambda t_i)] \quad , \qquad (1)$$

where φ is the particle flux, σ is the activation cross section, and $N_0 = N \cdot P \cdot W/M$, is the number of atoms in the target element, with $N = 6.022 \times 10^{23}$, the Avogadro constant, P the isotopic abundance, M the atomic mass of target element, and W the weight of target element.

The expression in brackets is the correction factor for decay during irradiation, where t_i is the irradiation time, $\lambda = \ln 2/T_{1/2}$ is the decay constant, and $T_{1/2}$ is the half life of the radioactive nuclei.

The saturation activity, A_∞, is the asymptotic value achieved, within 1%, at about seven times the half life:

$$A_\infty = \varphi \cdot \sigma \cdot N_0 \ . \qquad (2)$$

As the sample activity is measured by a spectrometer at a time t_e (elapsed time) after the end of the irradiation and during a time t_c (counting time), two more factors have to be taken into account:

a) a factor depending on the elapsed time t_e:

$$\exp\,(-\lambda \cdot t_e) \quad , \qquad (3)$$

b) a factor depending on the counting time t_c:

$$\overline{A} \cdot \lambda \cdot t_c / [1 - \exp(-\lambda \cdot t_c)] \ , \tag{4}$$

where $\overline{A}$, the activity measured by the spectrometer, is given by:

$$\overline{A} = \text{counts}/[t_c \cdot \eta\% \cdot \varepsilon\%] \ , \tag{5}$$

η being the emission probability and e the detection efficiency of the HPGe(p)–γ spectrometer.

Combining all the previous expressions:

$$\begin{aligned} A_\infty &= \overline{A} \cdot \lambda \cdot t_c \cdot \exp(\lambda \cdot t_e) / \\ &\quad \{[1 - \exp(-\lambda \cdot d_c)] \\ &\quad [1 - \exp(-\lambda \cdot t_i)]\} \ . \end{aligned} \tag{6}$$

The flux expression is then given by

$$\begin{aligned} \varphi &= A \cdot \lambda \cdot t_c \cdot \exp(\lambda \cdot t_e) \cdot M / \\ &\quad \{N_A \cdot P \cdot W \cdot \sigma \cdot \\ &\quad [1 - \exp(-\lambda \cdot t_c)] \\ &\quad [1 - \exp(-\lambda \cdot t_i)]\} \end{aligned} \tag{7}$$

and the fluence is the flux times the irradiation time t_i, hence

$$\Phi = \varphi \cdot t_i \ . \tag{8}$$

3.2. Fluence from Aluminium foils

The production of ^{24}Na from ^{27}Al [$^{27}Al(\pi^{\pm}, xN)^{24}Na$] was used to measure the fluence of π^+ and π^- in the energy range of about 50–350 MeV. ^{24}Na decays through β and γ emissions. The ^{24}Na activities were measured by a HPGe(p)–γ spectrometer selecting the 1369 keV γ-rays with a resolution of about 2.0 keV at FWHM. The collected spectra were computed by the INTERGAMMA code, giving sample activity. The activities at saturation and, then, the corresponding fluences, were calculated by using Eqs. (7) and (8) with the reaction cross-sections obtained from Ref. [2].

3.3. Fluence from Carbon foils

Graphite foils were used to provide a cross-check of the pion fluence values obtained by Al foils. The graphite foils were used in tandem with Al foils. The activity of ^{11}C produced by the $^{12}C(\pi^{\pm}, xN)^{11}C$ reaction was measured by detecting the 511 keV γ-ray decay with the spectrometer mentioned above. The cross-section is taken from Ref. [2]. Due to the frequent beam stops and short half life of ^{11}C (20.39 minutes), graphite foils were not routinely used. The results obtained with Al and C were in agreement to within 5%.

3.4. Fluence from Indium

^{115}In disc shaped samples were used to detect the neutron contamination around the pion beam.

The neutron activation technique based on the $^{115}In(n, n')^{115}In^m$ reaction is well suited for fluence measurements of neutrons with an energy above 500 keV for several reasons:

- the activation cross-section is large, and well known [3];
- the threshold at about 500 keV prevents activation by low-energy neutrons;
- the half-life of 4.50 hours is convenient for the periods of irradiation considered;
- the activity of $^{115}In^m$ is determined by its 336 keV gamma ray decay. The technique based on the $^{115}In(n, \gamma)^{116}In^m$ reaction has been also used to detect thermal neutrons. The activity of $^{116}In^m$ is measured by the detection of 416.9, 1097.3 and 1293.5 keV gamma rays.

The ^{115}In discs were located on the Y and Z axis, at 5 cm from the beam line (See Fig. 3).

4. DOSIMETRIC MEASUREMENTS

Dosimetric measurements were performed to evaluate the pion doses in the beam and the gamma doses around it.

4.1. Thermoluminescent dosimeters (TLD)

Thermoluminescent materials have the capability of storing part of the energy absorbed with sufficient stability when exposed to a radiation field. Impurities intentionally added to a host lattice create new energy levels within the band gap between the valence and conduction bands. These new levels can act as traps for electrons and/or holes created during material irradiation, preventing prompt recombination. If after irradiation the material is heated up to an adequately high temperature, the trapped charges will receive sufficient thermal energy to be liberated.

This liberation provokes recombinations that restore the pre-irradiation lattice conditions. The energy liberated upon heating (thermoluminescence measurement or readout) is converted into light proportional to the dose absorbed during irradiation.

The TLDs used in the present experiment are based on lithium fluoride activated by Mg and Ti. They are produced by Harshaw Co. (USA) in solid form (ribbon) with the commercial name TLD-700. They were used to estimate the gamma ray contamination during the pion irradiations. The dimensions of the TLDs are $3 \times 3 \times 0.9$ mm^3. They were located in two different positions along both the Y and Z axes, at 10 and 28 cm from the beam direction, as shown in Fig. 3.

4.2. Polymer-Alanine Dosimeters (PAD)

In Electron Spin Resonance (ESR) dosimetry, the ionizing radiation leads to the production of paramagnetic centres, which give rise to a characteristic ESR signal. The number of paramagnetic centres, and in turn the amplitude of the corresponding ESR signal, is proportional to the dose. In the present case, standard polymer-alanine dosimeters (PAD, 4.8 mm in diameter and 30 mm long) are cut from the Elcugray cable which uses ethylene-propylene rubber as a binder. The PADs were positioned on the back of the irradiation box to measure the pion dose. After irradiation they were read out by the ESR technique on a Varian E-3 spectrometer.

5. RESULTS

Because the pion beam size varied strongly along the beam direction (Fig. 2), several Al foils were used to measure the fluence along the irradiation box. During the irradiation runs, the Al foils were located at the relevant positions in front of each group of silicon detectors. The fluence obtained from these foils can therefore be used directly as a measure of the fluence received by the silicon detectors. To get more accurate measurements, the foils to be counted were sandwiched between two foils of the same material so that recoils leaving the foil are replaced by recoils from the cover foils. It must be noted that the duration of an irradiation is calculated from the start and stop times and does not take into account periods when the beam was off. In fact, the beam-off periods were always very short compared with the half-life of ^{24}Na (15 hours), so that no correction to the flux calculations was necessary. Figure 4 shows the flux normalized to the cyclotron intensity as a function of the position along the beam line for various π^+ momenta. The maximum flux was obtained in the region of 300–350 MeV/c. The momentum of 350 MeV/c was selected for the high fluence accumulation runs. This momentum is close to the energy of the Δ resonance, which could enhance the damage induced by pions in silicon [4, 5].

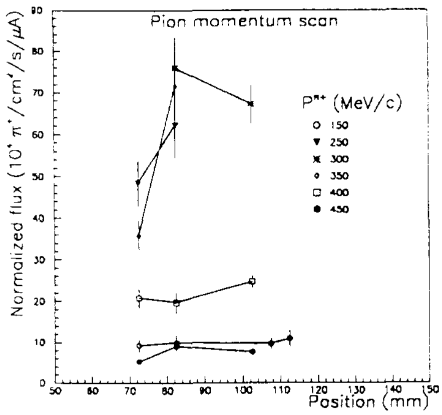

Figure 4. Normalized flux as a function of the irradiation positions along the beam line at different pion momenta

5.1. π^+ beam profile at 350 MeV/c

Figure 5 shows the average flux as measured with Al foils for the 350 MeV beam as a function of various positions along the irradiation box. The flux strongly decreases from the front to the back of the box. The beam density obtained from the XY profile chamber (see section 2) is shown in the same figure. Both measurements are in very good agreement.

5.2. Pion fluence calibration during irradiation runs

The pion accumulation runs were performed at a momentum of 350 MeV/c, up to fluences of $\sim 10^{14}$ cm^{-2} for π^+ and 10^{13} cm^{-2} for π^-.

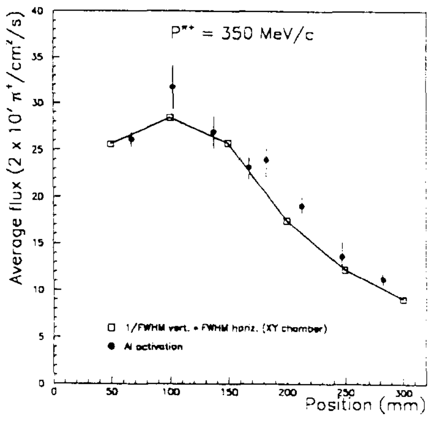

Figure 5. Comparison of the longitudinal beam profile at a momentum of 350 MeV/c as obtained by the X–Y chamber and by the Al activation

It would not have been possible to have an aluminium foil in front of each irradiated silicon detector due to the amount of time needed for activity measurements. Therefore, four aluminium runs were performed during the π^+ accumulation period. For each run, Al foils of the same area were located in front of each group of silicon detectors. The Al-runs were then used to calibrate the ionization chamber (see Chapter 2). Figure 6 shows an example of the fluence measured with

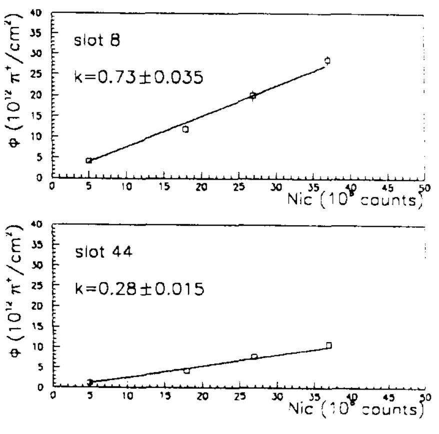

Figure 6. Examples of calibration factors deduced from Al fluence measurements versus ionization chamber counts

the Al foils as a function of the ionization chamber counts for two different positions in the irradiation box. The points were fitted and a calibration factor k was obtained at a given position in the irradiation box. The calibration factors can then be used to calculate the fluence, Φ, received by any silicon detector irradiated during the accumulation runs using the equation

$$k_j = \Phi_j / N_{ic} \quad , \tag{9}$$

where j denotes the longitudinal positions of the detectors, Φ_j is the fluence at the position j received by each Al foil, and N_{ic} is the number of counts from the ionization chamber.

Figure 7 shows the flux as a function of the Si detector irradiation position in the box, for the four succesive runs.

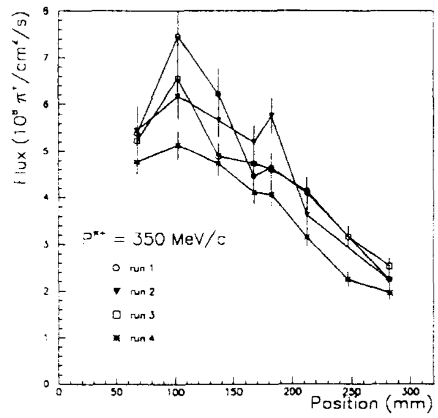

Figure 7. Positive π flux as a function of Si-detector irradiation positions for succesive runs

A similar calibration of the ionization chamber was performed for the negative pion accumulation run.

5.3. Results from Indium activation

The activation of ^{115}In allowed the neutron contamination around the positive pion beam line to be measured. The activation of ^{115}In produces two isotopes (see Table 1). Considering the neutron energy at which the two nuclear reactions can be produced and using the corresponding cross-sections, the thermal and fast neutron contaminations around the π^+ beam were estimated.

At 5 cm from the beam, the thermal and fast neutron contaminations varied respectively from 0.3 to 0.8% and from 0.2 to 0.5% of the positive pion flux.

5.4. Results from the dosimetry

The 350 MeV/c π^+ dose rate measured by the Alanine dosimeters (PAD) located in the beam was 337 ± 72 Gy/h. The thermoluminescent dosimeters (TLD), measured the γ dose. At 10 cm from the beam axis a dose rate of 5.0 ± 0.8 Gy/h was obtained. At 28 cm the dose rate fell to 0.70 ± 0.03 Gy/h.

6. CONCLUSIONS

The Aluminium activation technique permitted the $\pi^\pm$ fluences to be measured to within 5%. As a result, the ionization chamber was calibrated to measure fluence as a function of the beam intensity. The Al activation fluence measurements were extensively used by the SIRAD collaboration at PSI. The use of different types of radiation detection materials, such as Indium, thermoluminescent and alanine dosimeters, was very useful to determine the n and γ contamination during the pion irradiation runs. With the Indium, a maximum neutron contamination of 0.8% was estimated; the thermoluminescent detectors (TLD) gave a γ dose rate of 5 Gy/h at 10 cm and 0.7 Gy/h at 28 cm from the beam axis. Finally, the combined use of various kinds of dosimeters proved to be necessary to properly characterize the beam and its environment.

ACKNOWLEDGEMENTS

The authors wish to thank PSI for providing beam time (R. Horisberger), beam set-up (R. Frosch), beam diagnostic instrumentation and installation (K. Gabathuler) and gamma spectrometry (A. Janett).

REFERENCES

1. A. Van Ginneken, Tech. Rep. FN-522, Fermi Nat. Acc. Lab. (1989).
2. Landolt-Bornstein, Production of Radionuclides at Intermediate Energies, Gr. I, Vol. 13, Subvol. D, E (1994).
3. V. McLane, C.L. Dunford, P.F. Rose, Neutron Cross Sections, Vol. 2 (1987) N.Y., Academic Press, Inc.
4. M. Huhtinen and P. Aarnio, Nucl. Instrum. Methods **A335** (1993) 580.
5. Review of Particle Properties, Phys. Rev. **D45** Part II (1992), S1.